



Carpaine: Multitarget docking for its Antiproliferative Potential on CHO-k1 Human Ovarian Carcinoma



CrossMark

Yasmine M. Mandour^a, Ibrahim A. Saleh^b, Sally A. Abdel-Halim^b, Mona M. AbdelMohsen^{b*}

^aSchool of Life and Medical Sciences, University of Hertfordshire hosted by Global Academic Foundation, New Administrative Capitol 11578, Cairo, Egypt.

^bChemistry of Medicinal Plants Department, National Research Centre, 33 El Bohouth st. (Former El Tahrir St.), Dokki, Giza P.O.12622, Egypt.

Abstract

Ovarian cancer (OC) accounts as a common critical malignant tumor among female diseases. Among numerous drug resources, botanical compounds identified and isolated from plants have unique advantages due to their potential as chemotherapeutic drugs for cancer treatment. The aim of the study is to apply innovative extraction technique to increase carpaine obtained yield and investigate its antiproliferative activity on ovarian cancer. This work reports the extraction of carpaine from the leaves of *Carica papaya* using microwave-assisted extraction (MAE). Quantitative analysis of carpaine in the ethanol extract was conducted using HPLC with UV detection. The antiproliferative activity of extracted carpaine was investigated on CHO-K1 cell line (ovarian carcinoma) by MTT assay. Molecular modeling was employed to check the binding mode of carpaine with the 20S proteasome enzyme. Carpaine was detected in the alkaloid residue at 304 nm with retention time 36.50 min and the HPLC analytical methodology for standard curve was developed and validated to quantify carpaine as 0.29% of the dried leaves of *Carica papaya*. It was highly active against the human ovarian cancer cell line, CHO-K1, with IC₅₀ value of 28.40±3.2 µg/ml compared to vinblastine sulfate, the reference standard, which gave IC₅₀ value of 9.65±0.74 µg/ml. Molecular study emphasized the influential carpaine fitting in the binding site of 20S proteasome enzyme suggesting it is the prospective key player for carpaine's observed anti-ovarian cancer activity. These results suggest important guidance for the potential pathway of carpaine as an effective *Carica papaya*'s extract component for the prevention or amelioration of cancer. Consequently, it is highly expected to be utilized as functional food contributing to the preservation and promotion of human health.

Keywords: Carpaine; Microwave-assisted extraction; Ovarian cancer; Molecular docking.

Introduction

Ovarian cancer is a prevalent cancer in women accounting for a high percentage of all malignancies, thus threatening female reproductive health [1, 2]. Treatment depends greatly on the stage of its spread. Side effects of the currently used drugs, impairment of patient's life with long treatment and fear of developing drug resistance among cancer cells impose a great challenge in the treatment of cancer [3]. Henceforth, a healthy diet along with natural products as new treatment may prove beneficial in the control of ovarian cancer. Plant extracts rich in secondary metabolites have been used as a remedy for various disorders due to their unique advantages and potentials in multitarget functions, long application history and availability [4]. However, isolation of the main bioactive constituents from medicinal plants and their subsequent use as drugs in a pure form is a challenging

approach. Carpaine, a macrocyclic lactone, has been reported to have anticancer activity on various cell lines [5]. It is the main active constituent in *Carica papaya*, which is commonly called paw paw, an effective fruit used traditionally by many countries due to its nutritional and health benefits [6]. Extraction is one of the critical steps in achieving complete recovery of targeted compounds. Recent innovative extraction techniques that emphasize on speed and efficiency in retaining bioactive compounds, while optimizing parameters significant in economic terms are essential. Microwave-assisted extraction (MAE) which represents a reliable alternative method to conventional maceration has been used to increase the yield in shorter time using less solvent [7]. Computational methods are commonly used to propose an underlying mechanism explaining the observed anticancer activity of natural compounds [8].

*Corresponding author e-mail: monaamohsen@yahoo.com; (Mona M. AbdelMohsen).

Receive Date: 02 February 2023, Revise Date: 12 April 2023, Accept Date: 02 May 2023

DOI: 10.21608/EJCHEM.2023.182124.7360

©2023 National Information and Documentation Center (NIDOC)

The objective of the present study is to apply an innovative extraction technique; microwave-assisted extraction on *Carica papaya* leaves to boost carpaine content in maximum yield which is quantified using HPLC. Furthermore, the anti-cancer activity of carpaine was investigated on CHO-K1 cell line (ovarian carcinoma) by MTT assay and molecular docking analysis was performed to explain its observed anti-ovarian cancer activity.

Materials and methods

Plant material and extract preparation

Fresh leaves of *Carica papaya* Linn. were collected from Al-Aziziyah Gardens Resort, Cairo Alexandria Desert Road, Giza under the supervision of Dr. Kamal Zayed, professor of Ecology, Faculty of science, Cairo University (complying with national guidelines). The collected leaves were dried in an air oven at 40 °C, grounded using an electric mill into coarse powder and kept in tightly closed containers. A voucher specimen was kept at the NRC herbarium (No. 3237). Powdered leaves (1 kg) were extracted by 80% aqueous ethanol using a monomode microwave apparatus (MAE), with focused system (CEM Corporation, Matthews, NC, USA; model MARS 240/50, No. 907511, frequency 2450 MHz) to provide continuous non-pulse heating on a single cavity in which the sample was placed. Extraction time took 20 min, temperature was set at 60 °C with a radiation output at 800 W power [9]. After the extraction time, the vessel was allowed to cool at room temperature, and the extract was filtered and evaporated at 50°C under reduced pressure using a rotary evaporator. For the preparation of the crude alkaloids, the residue of the extract was dissolved then taken with 2N hydrochloric acid, kept overnight in a refrigerator. Then it was filtered and extracted with successive portions of petroleum ether to remove fat materials. The remaining aqueous acidic solution was shaken with excess zinc dust, then filtered. The filtrate was rendered alkaline (pH 10, using pH meter) with concentrated ammonium hydroxide (pH of 11.63). The total alkaloids were extracted with chloroform. The collected chloroform layers were pooled and evaporated to dryness under reduced pressure at 45 °C. The pale yellowish brown residue obtained, was dissolved in acetone and left overnight to give pure crystals which were analyzed and identified using ESI /MS and NMR Joel-500MHz for ¹H-NMR as carpaine.

Preparation of standard solution and crude alkaloid extract

Identified carpaine was used as an analytical standard for high performance liquid chromatography (HPLC). A stock solution of 1 mg/mL was prepared in ethanol and applied as a standard. Standard solutions at concentrations of 5, 10, 15, 20 µg/mL were prepared

by serial dilution of the stock solution, and 20 µL from each was used for plotting analytical chromatograms to obtain the standard curve for carpaine. For quantitation of carpaine in ethanol extract of the leaves, the alkaloid residue was dissolved, transferred to an Eppendorf tube and filtered through 0.45 µm micro-filter before HPLC analysis.

HPLC Analysis

Standard concentrations were injected into HPLC system to obtain the standard calibration curve. Analyses were accomplished by HPLC system using a Column: Xterra RP 4.6x250 mm, 5µm at ambient temperature using linear gradient at a flow of 0.8 mL/min with A (acetonitrile) and B (ammonium acetate, 0.05 mol/L, pH 8.5). The peaks were detected at 304 nm as previously described [10].

Cytotoxic activity against cancer cell line

All materials and reagents for the cell cultures were purchased from Lonza (Verviers, Belgium). CHO-K1 cell line (ovary carcinoma) were obtained from VACSERA Tissue Culture Unit, Giza, Egypt. The cell lines were kept as monolayer culture in Dulbecco's modified Eagle's medium (DMEM) supplied with 10% FBS, 4mM L-glutamine, 100 U/mL penicillin, and 100µg/mL streptomycin sulfate. The monolayers were maintained at 70–90% confluence using a trypsin- EDTA solution. The cells were allowed to incubate in a humidified atmosphere at 37 °C with 5% CO₂. The cytotoxic activity of carpaine was measured by MTT assay, and vinblastine sulfate was applied as reference standard [11, 12]. Cytotoxicity was specified according to the percent cell viability using MTT assay, and half maximal inhibitory concentration (IC₅₀) was calculated from the growth inhibition curve.

Statistical analysis

The IC₅₀ values (concentration of sample causing 50% loss of intact cells of the control vehicle) were presented as mean values ± (SD) and were calculated using the concentration-response curve appropriate to the non-linear regression model using GraphPad Prism® v6.0 software (GraphPad Software Inc., San Diego, CA, USA).

Computational study of carpaine

Protein and ligand preparation

From the literature, PARP-1, MDM2, VEGFR and 20S proteasome were chosen as drug targets for ovarian cancer [13]. The X-ray crystal structure of PARP-1 and co-crystallized ligand (PDB ID: 7AAD) [14], MDM2 and co-crystallized ligand (PDB ID: 4HG7) [15], VEGFR-2 and co-crystallized ligand (PDB ID: 3WZE) [16] and 20S proteasome and co-crystallized ligand (PDB ID: 1JD2) [17] were availed from Protein Data

Bank. The proteins were set with the structure preparation wizard in MOE (version 2019.01) and saved as a mol2 file. The 3D structure of the compound (carpaine) was built and minimized using the MMFF94x force field in MOE using a gradient of 0.0001 kcal/mol Å.

Molecular docking

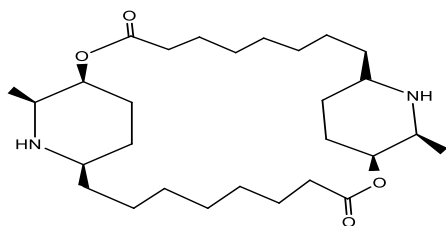
Docking was applied using GOLD (version 5.8) [18, 19]. Binding site residues were defined by specifying the inhibitors' crystal structure coordinates using the default cutoff radius of 6 Å, with the "detect cavity" option enabled. GOLD docking experiments were done using the ChemPLP scoring function. The search efficiency of the genetic algorithm was at 200% setting with the receptor kept rigid. A total of 50 complexes were created and clustered based on their RMSD with the threshold set at 0.75 Å using the complete linkage method. The best-ranked pose from the most populated cluster was chosen as the final pose. The quality of pose prediction was assessed by calculating the heavy atom RMSD between the docked poses and the original PDB coordinates of the cocrystallized ligand. The figures were set using PyMol (The PyMOL Molecular Graphics System, Version 2.0).

Molecular Dynamics Simulation

Molecular dynamics (MD) simulations were performed using the PMEMD.cuda code of the AMBER Molecular Dynamics package [20] following the same previously described protocol of minimization, heating, density equilibration and production [21]. The system was first heated to 300K for 20 ps then underwent subsequent density equilibrations for 200 ps before conducting a 100 ns production run. The trajectories were analyzed using CPPTraj [22]. Plots and visual inspection of the trajectories were performed using XMGrace [23] and VMD [24], respectively.

Results

Extraction, isolation and identification of carpaine
MAE produced a high extract yield (18.75 %). Consequently, the crude alkaloid content was high (0.35 %). Carpaine was isolated as pure crystals from the leaves of *Carica papaya* (Figure 1) and identified on the basis of spectroscopic analytic data which were confirmed by comparison with that reported in literature [25].



carpaine
Figure 1.

HPLC analysis

HPLC-DAD was applied for the quantification of carpaine in ethanol extract. Figure 2(A) depicts a representative chromatogram of the standard carpaine at 304 nm, the chromatographic retention time was 36.50 min, and 2(B) depicts the chromatogram demonstrating the detection of carpaine in the alkaloid residue under the optimized conditions. Quantitation was achieved against a standard curve of carpaine obtained from the analytical chromatograms at 304 nm. The linear regression data from the calibration curve was plotted over the range of 5- 20 µg/ml, $r^2 = 1$. Quantitative analysis of purified carpaine by HPLC specified that carpaine was the main alkaloid with 83% of the crude alkaloid residue extracted from *Carica papaya* leaves.

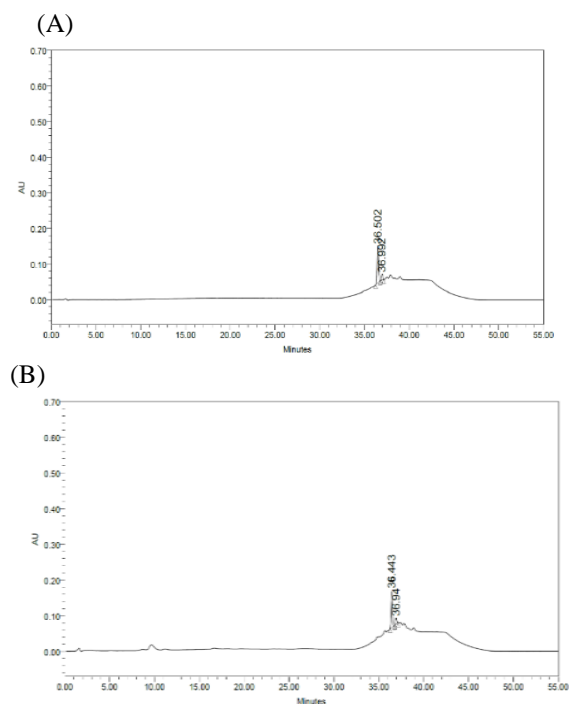


Figure 2. HPLC chromatogram of (A) carpaine, (B) crude alkaloid of MAE.

Cytotoxic activity

The cytotoxic activity of carpaine against CHO-K1 cell line (ovary carcinoma) was measured by MTT assay. The IC_{50} values were calculated using the concentration-response curves as demonstrated in Figure 3. The results showed high activity with IC_{50} value 28.40 ± 3.2 µg/ml for carpaine, while vinblastine sulfate, the reference standard, gave IC_{50} value of 9.65 ± 0.74 µg/ml.

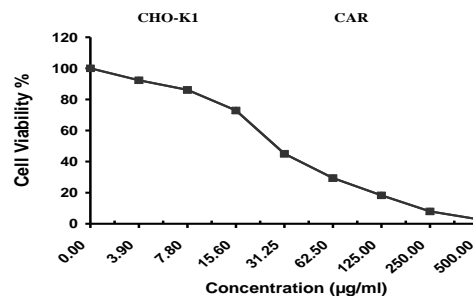
Molecular docking

In an attempt to explain the observed anti-ovarian cancer activity of carpaine, multitarget docking was performed to search for candidate molecular targets. The main therapeutic targets for ovarian cancer

considered in this study were human PARP-1, MDM2, VEGFR-2 and yeast 20S proteasome with their three-dimensional structures availed from protein data bank with the PDB codes: 7AAD [14], 4HG7 [15], 3WZE [16] and 1JD2 [17] respectively. Carpaine's docked poses were visually examined and evaluated based on their docking scores and interactions with reported key residues in the protein's active site (Table 1). Carpaine revealed promising binding mode to 20S proteasome enzyme having the highest docking score. Accordingly, the binding mode of carpaine to 20S proteasome will be discussed in more details. The structure of 20S proteasome enzyme complexed with its non-covalent inhibitor TMC-95A (PDB: 1JD2) [17] was used to check the binding mode of carpaine as the non-covalent mode of inhibition is more relevant to that of carpaine. It is worth mentioning that the crystal structure of the eukaryotic yeast 20S proteasome is structurally similar to the mammalian 20S proteasome with the catalytic binding domain of the two species highly conserved. To validate the docking protocol, the cocrystallized TMC-95A was docked into the active site of the 20S proteasome enzyme (Figure 4A). All the resultant poses converged to a binding mode similar to that of the experimentally determined position with the best ranking pose having a root mean square deviation (RMSD) value of 1.43 Å. The binding orientation of TMC-95A is overall similar to known covalent substrate-like inhibitors where it appeared preferentially occupying the S1 -S4 subsites of 20S proteasome enzyme. Docking of carpaine in the active site of 20S proteasome showed it occupying the S3 and S4 subsites interacting with key residues similar to TMC-95A (Figure 4B). To further confirm the stability of carpaine/20S proteasome complex, a 100 ns MD simulation was conducted using the AMBER software package [20]. To check the simulation convergence, we examined the time evolution of root mean square deviation (RMSD) of each of carpaine and 20S proteasome. Figure 5A shows that the backbone atoms of 20S proteasome fluctuated at the start of the simulation and levelled off at around 2.5 Å after almost 20 ns. Similarly, carpaine showed some fluctuations and stabilized around 1.6 Å after almost 20 ns. Visual inspection of the resultant trajectory showed carpaine highly retained inside the active site of the enzyme, maintaining its docked pose (Figure 5B). An average structure of the collected snapshots was generated, and the MD snapshot with the highest structural similarity with this average structure was chosen as the representative conformation. As shown in figure 5B, carpaine's binding mode in the average MD structure highly matched that of the X-ray structure confirming the docking results. Molecular docking and MD simulation studies of carpaine revealed its cyclic structure wrapping the

active site of 20S proteasome with its two piperidine rings contributing to its stable binding to the catalytic binding site (Figure 6A). The first piperidine ring fitted mainly in the S3 subsite and partially occupied the S4 subsite with its basic nitrogen forming a H-bond interaction with the backbone atoms of Thr21 and the sidechain of Ser20 (Figure 6B) which were maintained in 69% and 50% of the MD trajectory snapshots, respectively (Table 2). Moreover, the two oxygen atoms of its adjacent ester group acted as H-bond acceptors forming interactions with the side chain of Ser20 and the backbone atoms of Ala49, maintaining these interactions in 44% and 31% of the MD trajectory snapshots, respectively, and in analogy to P4 of TMC-95A in addition to an extra interaction with the acidic sidechain of Asp120. The other piperidine ring fitted outside the pocket with its basic nitrogen forming H-bond interactions with the backbone atoms of Ala27 and the adjacent ester group involved in a H-bond interaction with the sidechain of Ser364. However, the interactions of this second piperidine ring and its adjacent ester group were maintained in only 15% and 12% of the sampled snapshots, respectively implying a higher importance of the first piperidine ring in stabilizing carpaine's binding mode. Altogether, the highly stable binding mode of carpaine with its favorable interactions suggest 20S proteasome enzyme to be a key player for carpaine's observed anti-ovarian cancer activity.

A



B

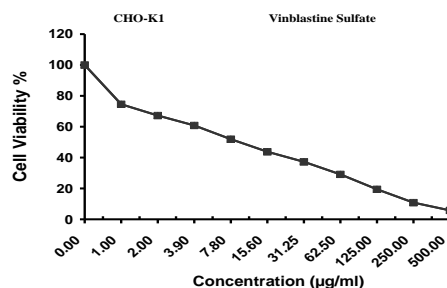
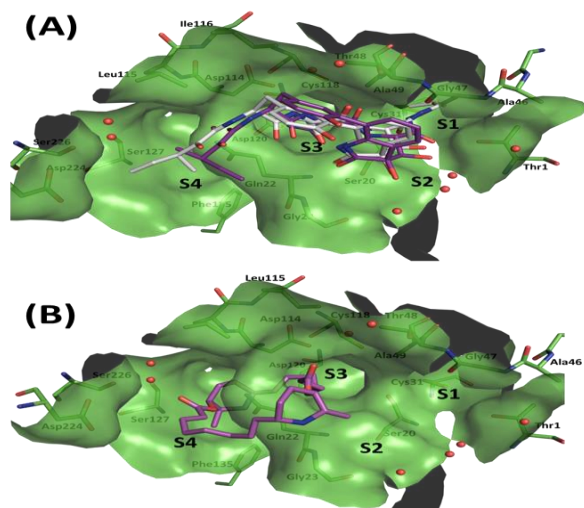
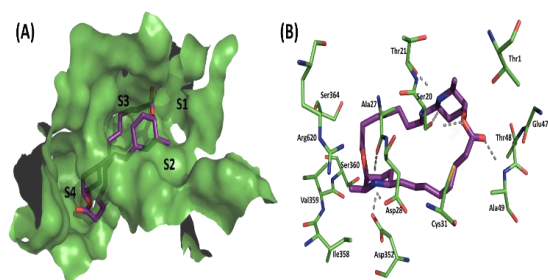
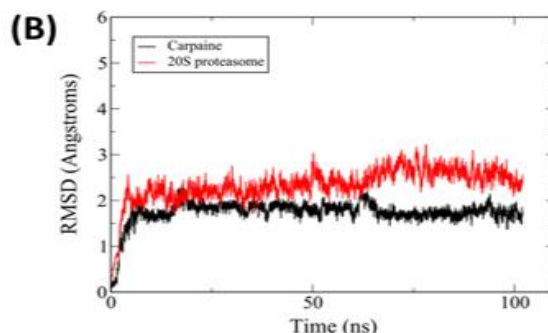
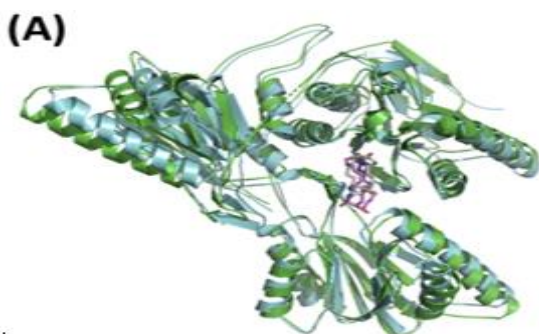


Figure 3. The concentration-response curves of A: carpaine; B: vinblastine sulfate (Reference Standard).

Table 1. ChemPLP scores of docked pose of carpaine with the respective protein drug target.

Protein target	ChemPLP score
20S proteasome	58.08
PARP-1	48.96
MDM2	54.03
VEGFR-2	-223.99

**Figure 4. Surface representation of the binding pocket of 20S proteasome enzyme (PDB: 1JD2). (A) Overlay of the docked pose (magenta) and PDB coordinates 2F71 (grey) of TMC-95A. (B) Docked pose of carpaine (magenta).****Figure 5. Plots of root-mean-square deviations of the entire trajectory consisting of structures sampled in intervals of 10 ps. The plot depicts RMSD values based on (A) protein backbone atoms and (B) ligand heavy atoms between the trajectory frames and the starting geometry.****Figure 6. Binding mode of docked pose of carpaine (magenta, sticks) in the active site of 20S proteasome (PDB: 1JD2) (green) (A) Surface representation of the binding pocket of 20S proteasome enzyme (B) Binding mode of carpaine showing its interactions with the active site residues.****Table 2. Protein-ligand interactions of carpaine's docked pose with the respective protein drug target.**

Type of interaction	Main interacting amino acid	Length of the bond	Role of the ligand in case of H-bond interaction
20S proteasome			
H-bond	Val126	2.81	H-donor
H-bond	Gln22	2.85	H-donor
H-bond	Asp120	3.38	H-donor
H-bond	Asp114	3.04	H-donor
PARP-1			
H-bond	Gln763	2.88	H-donor
H-bond	Glu988	2.64	H-donor
H-bond	Glu988	2.96	H-donor
Ionic	Glu988	2.97	
Ionic	Glu988	2.64	
MDM2			
H-bond	Leu840	3.30	H-donor
H-bond	Asn923	2.70	H-acceptor
VEGFR-2			
H-pi	His96	3.62	H-donor

Discussion

Medicinal plants role in treating ovarian cancer is inevitable. Conventionally, plant-derived natural products are considered to be auxiliary nutritional supplementary as a part of an initial treatment, an option for maintenance therapy, or to improve multiple-drug sensitivity, thus reducing the tumor and the metastatic burden of ovarian cancer. Plant-derived anti-ovarian cancer agents are effective inhibitors of cancer cells lines, making them in high demand as staple drugs for treatment and prevention, the new technologies are emerging to expand the area further for novel therapies to treat and prevent this life-threatening disease [26, 27, 28]. Accordingly, investigating the structure generalities and specialties of effective components deciphering the structure–activity relationship may contribute to understanding the detailed pharmacology and pharmacology, which could be the point cuts of enhancing the

bioavailability in human bodies, and to further develop targeted therapeutic drugs and reduce side effects in the breakthrough of ovarian cancer treatment.

In our study, carpaine was extracted in terms of green and environmental chemistry with 80 % ethanol using MAE technique which constitutes one of the simplest and most convenient extraction processes employing tremendous amount of intracellular pressure produced due to microwave radiation, allowing the energy to be strongly absorbed by the plant matrices, causing complete rupture to the cell wall, and release of the active constituents into the surrounding solvent. Carpaine was isolated in a pure form, then analyzed quantitatively in the alkaloid residue by RP-HPLC using a diode array detector (DAD) at 304 nm. Typical calibration curve was prepared using serial dilutions of stock solution of purified carpaine (5- 20 µg/ml) and plotting peak area (y) against injected amount (x, µg). The content of carpaine was quantified as 0.29% DW of the dried leaves of *Carica papaya*. In continuation, to investigate the anti-proliferative activity of *Carica papaya* [29, 30] the activity of carpaine against CHO-K1 cell line (ovary carcinoma) was measured by MTT assay and it showed high activity with IC₅₀ value 28.40±3.2 µg/ml, while vinblastine sulfate, the reference standard, gave IC₅₀ value of 9.65±0.74 µg/ml. Components of papaya leaves along with the major component carpaine alkaloid were reported to reduce blood pressure and posse antitumor and antiplasmodial activity [31, 32, 33]. Molecular docking is a computer simulation mode for studying the binding process of ligands and receptors and the interaction mechanism between molecules. This network pharmacological path has been recommended for carrying out critical studies on the interactions between active compounds of natural products and diseases to seek drug targets [34, 35].

In this study, molecular docking revealed the potential of carpaine to bind to20S proteasome enzyme which is the key in its anti-ovarian activity. The two piperidine rings contributed to the stability of carpaine's binding to the catalytic binding site. The first piperidine ring appeared popping out of S3 subsite and forming a H-bond interaction with the sidechain of Gln22 in analogy to P4 of TMC-95A in addition to an extra interaction with the acidic side chain of Asp120. The other piperidine ring occupied the S4 subsite with its adjacent ester group involved in a H-bond interaction with Asp114 of S3 subsite mimicking the backbone N of P3 of the cocrystallized TMC-95A. These favorable interactions suggest 20S proteasome enzyme to be a key player for the observed anti-ovarian cancer activity of carpaine.

Conclusion

In this study, MAE appeared as valuable technique to obtain carparine rich extracts from the leaves of

Carica papaya. Carpaine showed considerable anti-proliferative effect on CHO-K1 human ovarian carcinoma cell line. Molecular docking studies focused on certain parts of pathways and molecular mechanisms suggested that 20S proteasome enzyme to be responsible for the observed anti-ovarian cancer activity of carpaine.

Abbreviations

PARP-1; poly (ADP-ribose) polymerase-1, MDM2; mouse double minute 2, VEGFR; vascular endothelial growth factor, RMSD; root mean square deviation PMEMD; particle mesh Ewald molecular dynamics, CPPT; central polypurine tract, AMBER; assisted model building with energy refinement.

Conflict of interest statement

There are no conflicts to declare.

References

- [1] Holschneider C.H. and Berek J.S., Ovarian cancer: epidemiology, biology, and prognostic factors. *Semin Surg Oncol*, **19**, 3-10 (2000).
- [2] Webb P.M. and Jordan S.J., Epidemiology of epithelial ovarian cancer. *Best Pract. Res. Clin. Obstet. Gynaecol.*, **41**, 3-14 (2017).
- [3] Heinzlmann-Schwarz V., Mészáros A.K., Stadlmann S., Jacob F., Schoetzau A., Russell K., Friedlander M., Singer G. and Vetter M., Letrozole may be a valuable maintenance treatment in high-grade serous ovarian cancer patients. *Gynecol Oncol.*, **148**, 79-85 (2018).
- [4] Mohamed, T.A., Elshamy, A.I., Abdel Tawab , A.M., AbdelMohsen, M.M., Ohta, S., Pare, P.W. and Hegazy, M.E.F., Oxygenated Cembrene Diterpenes from *Sarcophyton convolutum*: Cytotoxic Sarcococonvolutum A-E. *Mar Drugs*, **19**(9), 519 (2021).
- [5] Vien D.T.H. and Thao D.T., Preliminary findings on anticancer and lymphocyte stimulated activities of bioactive compounds extracted from Vietnam *Carica papaya* leaves. *Journal of Food Science and Engineering*, **3**, 447-452 (2013).
- [6] Yogiraj V., Goyal P.K., Chauhan C.S., Goyal A. and Vyas B., *Carica papaya* Linn: An overview. *Int. J. Herb. Med.*, **2**(5), 1-8 (2014).
- [7] AbdelMohsen M.M., Nazif N.M., Seif EL Nasr M.M., Microwave-assisted extraction of bio-active compounds (phenolics and alkaloids) from *Echinacea purpurea*". *International Journal of Pharmacy and Pharmaceutical Sciences*, **6** (9), 265- 268 (2014).
- [8] Gurung A.B., Ali M.A., Lee J., Farah M.A. and Al-Anazi K.M., Molecular docking and dynamics simulation study of bioactive compounds from *Ficus carica* L. with important anticancer drug targets. *PLoS ONE*, **16**(7), e0254035 (2021).
- [9] Saleh I.A., Vinatoru M., Mason T.J., Abdel-Azim N.S., Shams K.A., Aboutabl E.A. and Hammouda F.M., Extraction of silymarin from milk thistle (*Silybum marianum*) seeds—a comparison of

- conventional and microwave-assisted extraction methods. *J Microw Power Electromagn Energy*, **51**, 124-133 (2017).
- [10] Wang X., Hu C., Ai Q., Chen Y., Wang Z. and Ou S., Isolation and Identification Carpaine in *Carica papaya* L. Leaf by HPLC-UV Method. *Int. J. Food Prop.*, **18**, 1505-1512 (2015).
- [11] Mosmann T., Rapid colorimetric assay for cellular growth and survival: application to proliferation and cytotoxicity assays. *J. Immunol. Res.*, **65**, 55-63 (1983).
- [12] Sylvester P.W., Optimization of the tetrazolium dye (MTT) colorimetric assay for cellular growth and viability. *Methods Mol Biol.*, **716**, 157-168 (2011).
- [13] Lim H.J. and Ledger W., Targeted therapy in ovarian cancer. *Womens Health (Lond.)*, **12**, 363-378 (2016).
- [14] Ogden T.E.H., Yang J.-C., Schimpl M., Easton L.E., Underwood E., Rawlins P.B., McCauley M.M., Langelier M.F., Pascal J.M., Embrey K.J. and Neuhaus D., Dynamics of the HD regulatory subdomain of PARP-1; substrate access and allostery in PARP activation and inhibition, *Nucleic Acids Res.* **49**, 2266-2288 (2021).
- [15] Anil B., Riedinger C., Endicott J.A. and Noble M.E.M., The structure of an MDM2–Nutlin-3a complex solved by the use of a validated MDM2 surface-entropy reduction mutant. *Acta Cryst.*, **D69**, 1358-1366 (2013).
- [16] Okamoto K., Ikemori-Kawada M., Jestel A., König K., Funahashi Y., Matsushima T., Tsuruoka A., Inoue A. and Matsui J., Distinct Binding Mode of Multikinase Inhibitor Lenvatinib Revealed by Biochemical Characterization. *ACS Med. Chem. Lett.*, **6**, 89-94 (2015).
- [17] Groll M., Koguchi Y., Huber R. and Kohno J., Crystal structure of the 20 S proteasome: TMC-95A complex: a non-covalent proteasome inhibitor. *J. Mol. Biol.*, **311**, 543-548 (2001).
- [18] Jones G., Willett P. and Glen R.C., Molecular recognition of receptor sites using a genetic algorithm with a description of desolvation. *J. Mol. Biol.*, **245**, 43-53 (1995).
- [19] Jones G., Willett P., Glen R.C., Leach A.R. and Taylor R., Development and validation of a genetic algorithm for flexible docking. *J. Mol. Biol.*, **267**, 727-748 (1997).
- [20] Case D.A., Aktulga H.M., Belfon K., Ben-Shalom I.Y., Brozell S.R., Cerutti D.S., Cheatham T.E., Cisneros III, G.A., Cruzeiro V.W.D., Darden T.A., Duke R.E., Giambasu G., Gilson M.K., Gohlke H., Goetz A.W., Harris R., Izadi S., Izmailov S.A., Jin C., Kasavajhala K., Kaymak M.C., King E., Kovalenko A., Kurtzman T., Lee T.S., LeGrand S., Li P., Lin C., Liu J., Luchko T., Luo R., Machado M., Man V., Manathunga M., Merz K.M., Miao Y., Mikhailovskii O., Monard G., Nguyen H., O’Hearn K.A., Onufriev A., Pan F., Pantano S., Qi R., Rahnamoun A., Roe D.R., Roitberg A., Saguí C., Schott-Verdugo S., Shen J., Simmerling C.L., Skrynnikov N.R., Smith J., Swails J., Walker R.C., Wang J., Wei H., Wolf R.M., Wu X., Xue Y., York D.M., Zhao S., and Kollman P.A., *Amber*, University of California, San Francisco (2021).
- [21] Mandour Y.M., Zlotos D. P. and Alaraby S.M., A multi-stage virtual screening of FDA-approved drugs reveals potential inhibitors of SARS-CoV-2 main protease. *J Biomol Struct Dyn.*, **40**(5), 2327-2338 (2022).
- [22] Roe D.R. and Cheatham III T.E., PTRAJ and CPPTRAJ: Software for Processing and Analysis of Molecular Dynamics Trajectory Data. *J. Chem. Theory Comput*, **9**(7), 3084-3095 (2013).
- [23] Turner P. J., XMGRACE (Version 5.1.19). Beaverton, OR: Center for Coastal and Land-Margin Research, Oregon Graduate Institute of Science and Technology (2005).
- [24] Humphrey W., Dalke A. and Schulten K., VMD: visual molecular dynamics. *J. Mol. Graph.* **14**, 33–38 (1996).
- [25] Julianti T., DeMieri M., Zimmermann S., Ebrahimi S.N., Kaiser M., Neuburger M., Raith M., Brun R. and Hamburger M., HPLC-based activity profiling for antiplasmodial activity in the traditional Indonesian medicinal plant *Carica papaya* L. *J. Ethnopharmacol.* **155**(1), 426-34 (2014).
- [26] Cortez A.J., Tudrej P., Kujawa K.A. and Lisowska K.M., Advances in ovarian cancer therapy. *Cancer Chemother Pharmacol.* **81**, 17-38 (2018).
- [27] Handoussa H., AbdAllah W. and AbdelMohsen M., UPLC–ESI-PDA–Msⁿ profiling of phenolics involved in biological activities of the medicinal plant *Halocnemum strobilaceum* (Pall.). *Iranian Journal of Pharmaceutical Research*, **18**(1), 422- 429 (2019).
- [28] Lim H.J. and Ledger W., Targeted therapy in ovarian cancer. *Womens Health (Lond.)*, **12**, 363-378 (2016).
- [29] Palanisamy P. and Basalingappa K. M., Phytochemical analysis and antioxidant properties of leaf extracts of *Carica papaya*. *Phytochemical Analysis*, **13**(11), 58-62 (2020).
- [30] Maisarah A. M., Asmah R. and Fauziah O., Proximate analysis, antioxidant and anti-proliferative activities of different parts of *Carica papaya*. *Journal of Nutrition and Food Science*, **5**(1), 267 (2014).
- [31] Morimoto, C. and Dang, N., Compositions for cancer prevention, treatment, or amelioration comprising papaya extract. <https://patentimages.storage.googleapis.com/2b/6b/8f/b99f38f4a1abc1/US20080069907A1.pdf> (2006).
- [32] Sharma A., Bachheti A., Sharma P., Bachheti R.K. and Husen A., Phytochemistry, pharmacological activities, nanoparticle fabrication, commercial products and waste utilization of *Carica papaya* L.: A comprehensive review. *CRBIOT*, **2**, 145-160 (2020).
- [33] Singh S.P., Kumar S., Mathan S.V., Tomar M.S., Singh R.K., Verma P.K., Kumar A., Kumar S., Singh R.P. and Acharya A., Therapeutic application of *Carica papaya* leaf extract in the management of human diseases. *DARU J. Pharm. Sci.*, **28** (2), 735-744 (2020).
- [34] Abd El-Mohsen M.M., Rabeh M.A., Abou-Setta L., El-Rashedy A.A. and Hussein A.A., Marrubiin: a potent α -glucosidase inhibitor from *Marrubium alysson*. *International Journal of Applied Research in Natural Products*, **7** (1), 21-27 (2014).
- [35] Oulas A., Minadakis G., Zachariou M., Sokratous K., Bourdakou M.M. and Spyrou G.M., Systems bioinformatics: Increasing precision of computational diagnostics and therapeutics through Network-Based approaches. *Brief Bioinform*, **20**(3), 806-824 (2019).